Original Article
http://dx.doi.org/10.5115/acb.2011.44.3.226
pISSN 2093-3665 eISSN 2093-3673
Anatomy & Cell Biology acb

Co-localization of activating transcription factor 3 and phosphorylated c-Jun in axotomized facial motoneurons

Byung Gu Park[1], Jin Sook Lee[1], Ji Yong Lee[1], Dae Yong Song[2], Seong-Woo Jeong[3], Byung Pil Cho[1]
[1]Department of Anatomy, Yonsei University Wonju College of Medicine, Wonju, [2]Department of Anatomy and Neuroscience, Eulji University School of Medicine, Daejeon, [3]Department of Physiology, Yonsei University Wonju College of Medicine, Wonju, Korea

Abstract: Activating transcription factor 3 (ATF3) and c-Jun play key roles in either cell death or cell survival, depending on the cellular background. To evaluate the functional significance of ATF3/c-Jun in the peripheral nervous system, we examined neuronal cell death, activation of ATF3/c-Jun, and microglial responses in facial motor nuclei up to 24 weeks after an extracranial facial nerve axotomy in adult rats. Following the axotomy, neuronal survival rate was progressively but significantly reduced to 79.1% at 16 weeks post-lesion (wpl) and to 65.2% at 24 wpl. ATF3 and phosphorylated c-Jun (pc-Jun) were detected in the majority of ipsilateral facial motoneurons with normal size and morphology during the early stage of degeneration (1-2 wpl). Thereafter, the number of facial motoneurons decreased gradually, and both ATF3 and pc-Jun were identified in degenerating neurons only. ATF3 and pc-Jun were co-localized in most cases. Additionally, a large number of activated microglia, recognized by OX6 (rat MHC II marker) and ED1 (phagocytic marker), gathered in the ipsilateral facial motor nuclei. Importantly, numerous OX6- and ED1-positive, phagocytic microglia closely surrounded and ingested pc-Jun-positive, degenerating neurons. Taken together, our results indicate that long-lasting co-localization of ATF3 and pc-Jun in axotomized facial motoneurons may be related to degenerative cascades provoked by an extracranial facial nerve axotomy.

Key words: Facial nerve axotomy, ATF3, pc-Jun, Microglia, Neurodegeneration

Received June 1, 2011; Revised June 28, 2011; Accepted August 1, 2011

Introduction

Immediate early genes (IEGs) are induced in a fast and transient manner in the nervous system by various stimuli [1]. Many IEGs encode transcription factors that control specific target genes related to neuronal response effector functions [2]. Axotomy induces and activates several IEGs, including activating transcription factor 3 (ATF3) and c-Jun [3-5]. ATF3, a member of the cAMP-responsive element binding protein/activating transcription factor (CREB/ATF) family, is induced by various types of tissue damage including axotomy [4-7]. However, the functional significance of stress-induced ATF3 expression is unclear due to conflicting data. Several investigators have proposed that ATF3 plays a protective role in neuronal or non-neuronal cells [8, 9]. In contrast, others have suggested that ATF3 is involved in cell death [4, 10, 11].

CREB/ATF family members have a basic region/leucine zipper domain that mediates their heterodimerization. ATF3 forms heterodimers with Jun proteins to activate transcription of certain genes [12], but as a homodimer, it represses gene transcription [6]. Similar to ATF3, the role of stress-induced c-Jun activation is unclear. c-Jun signaling appears to be

Corresponding author:
Byung Pil Cho
Department of Anatomy, Yonsei University Wonju College of Medicine, 162 Ilsan-dong, Wonju 220-701, Korea
Tel: +82-33-741-0272, Fax: +82-33-742-1434, E-mail: bpcho@yonsei.ac.kr
*Byung Gu Park and Jin Sook Lee contributed equally to this work.

involved in either cell survival or death, depending on the cell type and specific circumstances. Induction of c-Jun may be involved in neuronal protection or regeneration [1, 13, 14]; however, activation of c-Jun is also found in degenerating and apoptotic neurons [15-18], in axotomized neurons [19], and in biopsies from patients affected with Alzheimer's disease [20] and multiple sclerosis [21].

We previously reported co-localization of ATF3 and phosphorylated c-Jun (pc-Jun) in the degenerating dopamine (DA) neurons of the substantia nigra pars compacta after medial forebrain bundle (MFB) transection [4]. We also demonstrated that activated and phagocytic microglia specifically adhere to various parts of degenerating DA neurons throughout the entire neurodegenerative process [4, 22-24]. These findings strongly support the concept that the putative ATF3/pc-Jun heterodimer is closely related to axotomy-induced neurodegeneration in the central nervous system (CNS). However, many studies have suggested that activation of ATF3 and/or c-Jun is involved in neuronal regeneration or protection in the peripheral nervous system (PNS), including the central extrinsic neurons such as facial motoneurons [1, 9, 13, 25].

An extracranial facial nerve axotomy may result in delayed neuronal cell death in adult rats [26-28]. This finding implies the presence of phagocytic microglia in the facial motor nucleus after axotomy, because microglia respond sensitively to diverse neuropathological factors, even to very subtle alterations in their microenvironment, such as an imbalance in ion homeostasis that precedes detectable pathological change [29]. However, several authors have reported no phagocytic microglia in the facial motor nucleus following an extracranial facial nerve axotomy in adult rats [28, 30, 31]. Therefore, the interaction between degenerating neurons and microglia should be carefully investigated to verify this contradiction and to understand the exact pathophysiology induced by an extracranial facial nerve axotomy. Additionally, as an extracranial facial nerve axotomy induces slow and long-lasting neurodegeneration [26, 27], it is necessary to analyze microglial behavior and function over an extended period of time.

This study was performed to elucidate the functional significance of stress-induced activation of ATF3 and c-Jun in axotomized facial motoneurons. We examined temporal and spatial profiles of these IEGs in the facial motor nucleus after an extracranial facial nerve axotomy in adult rats. We also investigated the survival rate and morphological changes of axotomized facial motoneurons up to 6 months. Morphological and immunophenotypical changes in microglia, as well as their spatial relationship with axotomized facial motoneurons, were carefully analyzed to assess the status and propagation of ongoing neurodegeneration.

Materials and Methods

Animal care and surgical procedures

Animal use and care protocols were approved by the Institutional Animal Care and Use Committee of Yonsei University at Wonju Campus, Wonju, Korea. Forty adult male Wistar rats (body weight, 250-300 g; Charles River Lab., Wilmington, MA, USA) were used. All efforts were made to minimize the number of animals required and to ensure minimal suffering of animals. Rats were housed with free access to food and water in a room maintained at constant room temperature (20-22°C) with a 12 : 12-hour light-dark cycle.

For the extracranial facial nerve axotomy, rats were deeply anesthetized with an intraperitoneal injection of ketamine (70 mg/kg body weight) and xylazine (8 mg/kg body weight), and the left facial nerve was exposed posterior to the left ear. The facial nerve was transected at a point 2.0 mm inferior to the stylomastoid foramen, and a 2.0 mm long fragment of the distal section was removed to avoid spontaneous union of the two separated parts of the nerve. After suturing of the skin, animals were kept on a heating plate at 37°C until they completely recovered. Animals were sacrificed at various time points between 3 days post-lesion and 24 weeks post-lesion (wpl). The contralateral side of the brain was used as the internal control, because the facial nerve does not cross the midline during its course to the PNS.

Retrograde tracing with FluoroGold

To examine the spatial relationship between activated microglia and degenerating facial motoneurons in detail, various parts of axotomized facial motoneurons were detected by retrograde tracing using FluoroGold (FG; Fluorochrome, Englewood, CO, USA) at 2 wpl. Under deep anesthesia, the proximal segment of the transected nerve end was carefully exposed, and 0.1% FG dissolved in 0.9% physiological saline was added to the segment. Then, the overlying skin was sutured, and the animals were kept on a heating plate at 37°C until they completely recovered. The animals were sacrificed 2

http://dx.doi.org/10.5115/acb.2011.44.3.226

days after the FG treatment.

Sample preparation and immunohistochemistry

All animals were deeply anesthetized as described above, and the thorax was opened. Animals were at first perfused transcardially with 100 ml of ice-cold 0.1 M phosphate buffer (PB; pH 7.4) containing 0.5% sodium nitrite and 10 U/ml heparin, then with 400 ml of 4% paraformaldehyde in 0.1 M PB. The brain was carefully removed from the skull and, based on the atlas of Paxinos and Watson [32], sliced into a block to contain the facial motor nucleus. The brain block was post-fixed for 12 hours in the same fixative and was infiltrated with 30% sucrose solution overnight at 4°C until it had submerged. The block was then rapidly frozen in 2-methylbutane chilled on dry ice and mounted in Tissue-Tek OCT compound (Sakura Finetechnical Co., Tokyo, Japan). Serial coronal sections of 40 μm thickness were obtained on a cryostat microtome (Leica Microsystems Inc., Wetzlar, Germany) and were distributed sequentially to a set of twelve tissue wells containing 0.1 M PB. After a brief wash with 0.1 M PB, the brain sections were transferred to another set of twelve tissue wells containing cryoprotection solution and were then stored in a freezer at a temperature less than -20°C until use.

The sections were washed three times with 0.1 M PB containing 0.9% sodium chloride and 0.1% Triton X-100 (PBST, pH 7.4) and were treated with 3% hydrogen peroxide for 15 minutes to suppress endogenous peroxidase activity. After washing with 0.1 M PBST, the sections were treated for 1 hour with 5% normal serum obtained from the same host species as the secondary antibody to reduce non-specific binding and were then incubated with primary antibodies diluted in 0.1 M PBST for 12 hours at 25°C.

The primary antibodies used were: rabbit polyclonal anti-ATF3 (1 : 500, Santa Cruz Biotechnology, Santa Cruz, CA, USA), rabbit polyclonal anti-pc-Jun (1 : 300, Ser 63, Cell Signaling Technology Inc., Beverly, MA, USA), rabbit polyclonal anti-FG (1 : 1,000, Chemicon, Temecula, CA, USA), mouse monoclonal anti-neuronal nuclei (NeuN; 1 : 500, Chemicon), mouse monoclonal anti-rat MHC II (1 : 500, OX6, Serotec, Oxford, UK), and mouse monoclonal anti-rat CD68 (1 : 500, ED1, Serotec). OX6 and ED1 were used to identify activated microglia: ED1 labels the lysosomal enzyme, which is upregulated in microglia during phagocytosis [33], and OX6 labels rat MHC class II, which is upregulated in activated microglia including those that are phagocytic [4, 22, 24, 34].

After the primary antibody incubation, the sections were washed three times with 0.1 M PBST and incubated for 2 hours with biotinylated goat anti-rabbit IgG (1 : 200, Vector Lab., Burlingame, CA, USA) for ATF3 and pc-Jun, or with biotinylated horse anti-mouse IgG (1 : 200, Vector Lab.) for NeuN and microglia markers. After three washes, sections were incubated with avidin-biotin-peroxidase complex (ABC; Vector Lab.) for 1 hour and treated with 0.05% 3,3'-diaminobenzidine tetrahydrochloride (DAB; Sigma-Aldrich, St. Louis, MO, USA) containing 0.01% hydrogen peroxide for 5 minutes to detect peroxidase activity. Sections were mounted on gelatin-coated slides, counterstained with 0.1% cresyl violet (Sigma-Aldrich), dehydrated through a graded ethanol series, cleared in xylene, and covered with coverslips using Permount.

Multiple immunohistochemistry

Multiple immunohistochemistry was performed as previously described [22]. Briefly, each labeling step was performed sequentially using the peroxidase ABC method, and possible cross reactions between immunological reactions against primary antibodies derived from the same host species were blocked using unconjugated Fab IgG. For double immunohistochemical labeling of ED1 (or FG) and OX6, sections were first stained with ED1 (or FG) using DAB-nickel (black reaction product; Vector Lab.), and then with OX6 using DAB (brown reaction product). Because the spatial relationship between activated microglia and damaged neurons could provide meaningful data on the outcome of neurons, some sections were triple-labeled with antibodies for pc-Jun, OX6, and NeuN. In such cases, sections were first stained with anti-pc-Jun antibody using DAB-nickel, then with OX6 using DAB, and finally with anti-NeuN antibody using VIP (purple reaction product; Vector Lab.).

Double immunofluorescence labeling

Co-localization of ATF3 and pc-Jun was examined by indirect immunofluorescence. Sections were first incubated with 10% normal goat serum for 1 hour, followed by an incubation with anti-pc-Jun antibody (1 : 30) for 12 hours at 4°C. After rinsing in PBS, Cy3-conjugated goat anti-rabbit IgG (1 : 250, Jackson ImmunoResearch Lab., West Grove, PA, USA) was applied for 2 hours at room temperature. Sections were rinsed and then incubated first with 10% normal rabbit serum for 1 hour and then with an excess of unconjugated Fab goat anti-rabbit IgG (1 : 20, Jackson ImmunoResearch

Lab.) for 1 hour to block the activity of the first antibody. The sections were then incubated with anti-ATF3 antibody (1 : 50) for 12 hours, biotinylated goat anti-rabbit IgG (1 : 200) for 2 hours, and FITC-conjugated avidin D (1 : 50, Vector Lab.) for 1 hour at room temperature. Finally, the sections were rinsed in PBS and mounted with Vectashield (Vector Lab.).

Cell count

The number of facial motoneurons was counted on coronal sections stained with cresyl violet. Two of 12 sets of samples were randomly chosen from each animal and were mounted on gelatin-coated slides after three washes with 0.1 M PB. After staining with 0.1% cresyl violet, the samples were dehydrated through a graded ethanol series, cleared in xylene, and covered with coverslips. Light photomicrographic images were acquired on a Nikon Optiphot microscope (Nikon Inc., Tokyo, Japan) fitted with a Nikon digital camera (DXM1200), using Nikon ACT-1 image capture software (ver. 2.2). These images were imported into Adobe Photoshop (ver. 7.0, Adobe Systems Inc., San Jose, CA, USA) and were adjusted for brightness and contrast to optimize photographic representation of the images obtained by the microscope. All neurons on both sides of the facial motor nucleus were counted with the analySIS (Olympus Soft Imaging

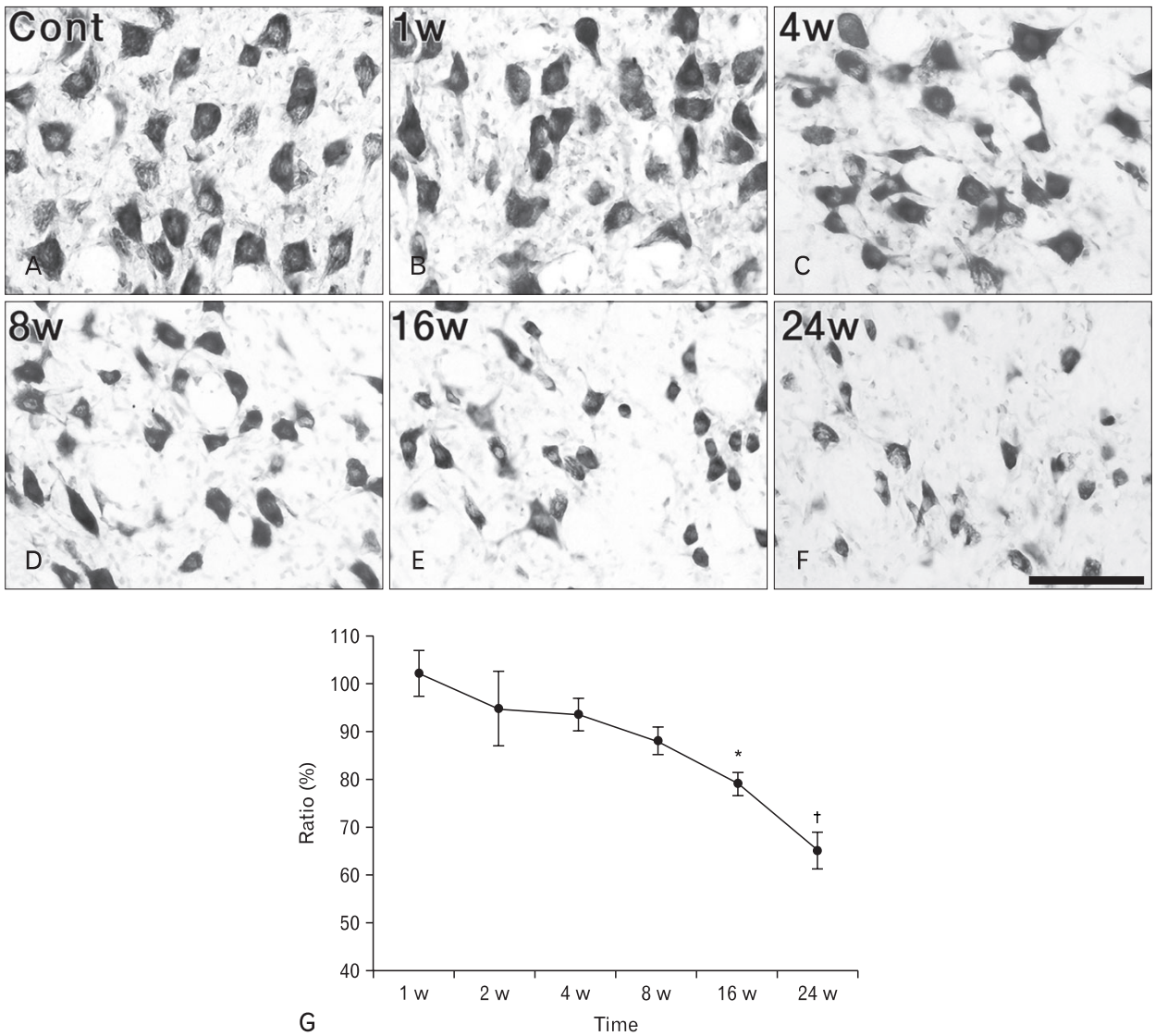

Fig. 1. (A-F) Facial motoneurons stained with cresyl violet on the contralateral (A) and ipsilateral (B-F) sides. Significant loss of facial motoneurons was clearly identified from 16 weeks (w) post-lesion (E, F). Cont, contralateral. Scale bar=100 μm (A-F). (G) Survival rates of ipsilateral facial motoneurons compared to the corresponding contralateral side. *P<0.05, †P<0.01.

http://dx.doi.org/10.5115/acb.2011.44.3.226

System, Münster, Germany) image analyzer system, and the percentages of ipsilateral facial motoneurons compared to the corresponding contralateral facial motoneurons were calculated. In addition, the number of ATF3- and pc-Jun-positive neurons in the ipsilateral facial motor nucleus was similarly counted using immunohistochemically stained coronal sections, and their percentages to the total number of facial motoneurons on the same side were obtained.

Data analysis

t-tests and a repeated-measures analysis of variance were performed to statistically analyze the number of facial motoneurons. An univariate analysis was also performed using an F-test in which the degrees of freedom were adjusted to a smaller value using Huynh-Feldt methods. A value of $P<0.05$ was considered statistically significant.

Results

Loss of facial motoneurons following the extracranial facial nerve axotomy

Following the extracranial facial nerve axotomy, the number of facial motoneurons gradually and consistently decreased until 24 weeks (Fig. 1). Compared to the corresponding contralateral facial motoneurons, survival rates of the ipsilateral neurons were 102.1%, 94.7%, 93.4%, 88.0%, 79.1%, and 65.2% at 1, 2, 4, 8, 16, and 24 wpl, respectively. The neuronal loss was not statistically significant until 8 wpl, but it became significant at 16 and 24 wpl (Fig. 1G). The shape and size of the ipsilateral neurons were similar to those of the contralateral neurons up to 4 wpl (Fig. 1A-C), but many neurons found at later time points showed shrunken morphology with a markedly reduced soma size (Fig. 1D-F).

Co-localization of ATF3 and pc-Jun in axotomized facial motoneurons

The ipsilateral facial motor nucleus revealed specific ATF3 and pc-Jun localization patterns, but neither ATF3- nor pc-Jun-positive neurons were found on the contralateral side (Fig. 2). The extracranial facial nerve axotomy triggered a prompt induction and activation of ATF3 and c-Jun in the nuclei of axotomized neurons, leading to the prevalence of ATF3- and pc-Jun-positive nuclei in the ipsilateral facial motor nucleus. The majority of ipsilateral facial motoneurons became ATF3- and pc-Jun-positive by 2 wpl, and the number of ATF3- and pc-Jun-positive neurons then decreased progressively. In general, the distribution patterns, as well as the temporal profiles of ATF3-positive neurons (Fig. 2B-F), were very similar to those of pc-Jun-positive neurons (Fig. 2H-L), but the number of ATF3-positive neurons was always greater than that of pc-Jun-positive neurons (Fig. 2M). The percentages of ATF3-positive neurons were 90.1% (1 wpl), 91.9% (2 wpl), 72.6% (4 wpl), 42.6% (8 wpl), 25.8% (16 wpl), and 21.0% (24 wpl) of the corresponding ipsilateral facial motoneurons. The percentages of pc-Jun-positive neurons were 73.7% (1 wpl), 82.2% (2 wpl), 64.2% (4 wpl), 26.2% (8 wpl), 9.1% (16 wpl), and 0.1% (24 wpl) of the corresponding ipsilateral facial motoneurons (Fig. 2M).

By 2 wpl, the size and shape of ATF3- and pc-Jun-positive neurons were very similar to those of the contralateral neurons (Fig. 2A-C, 2G-I). Thereafter, however, ATF3 and pc-Jun were found in neurons showing degenerative features, such as shrunken soma and condensed nuclei (Fig. 2D-F, 2J-L). From 8 wpl onward, ATF3 and pc-Jun were identified in the majority of small-sized degenerating neurons (arrowheads in insets of Fig. 2E, F, K, L), whereas ipsilateral neurons with normal size and morphology were both ATF3- and pc-Jun-negative (arrows in insets of Fig. 2E, F, K, L). Double immunofluorescence labeling demonstrated co-localization of ATF3 and pc-Jun in the same axotomized facial motoneurons in most cases, with the exception of a few cells that were exclusively ATF3- or pc-Jun-positive (Fig. 3).

Activated microglia in response to axotomy-induced neurodegeneration and their relationship with pc-Jun-positive facial motoneurons

Numerous OX6-positive microglia were found in the ipsilateral facial motor nucleus, whereas no OX6-positive microglia were present on the contralateral side (Fig. 4). A few OX6-positive microglia occurred in the ipsilateral facial motor nucleus as early as 1 wpl (Fig. 4B). Thereafter, the number of OX6-positive microglia increased dramatically until 8 wpl and then subsequently decreased progressively; however, the presence of OX6-positive microglia was still identifiable until 24 wpl (Fig. 4C-F). All OX6-positive microglia retained an "activated form," as they showed a ramified form with enlarged somas and thickened processes. Many of the OX6-positive, activated microglia tightly wrapped and/or stuck to the axotomized facial motoneurons throughout the entire duration of the experiment (arrows in insets of Fig. 4C, D, F): this phenomenon was particularly prominent at 8 wpl (Fig.

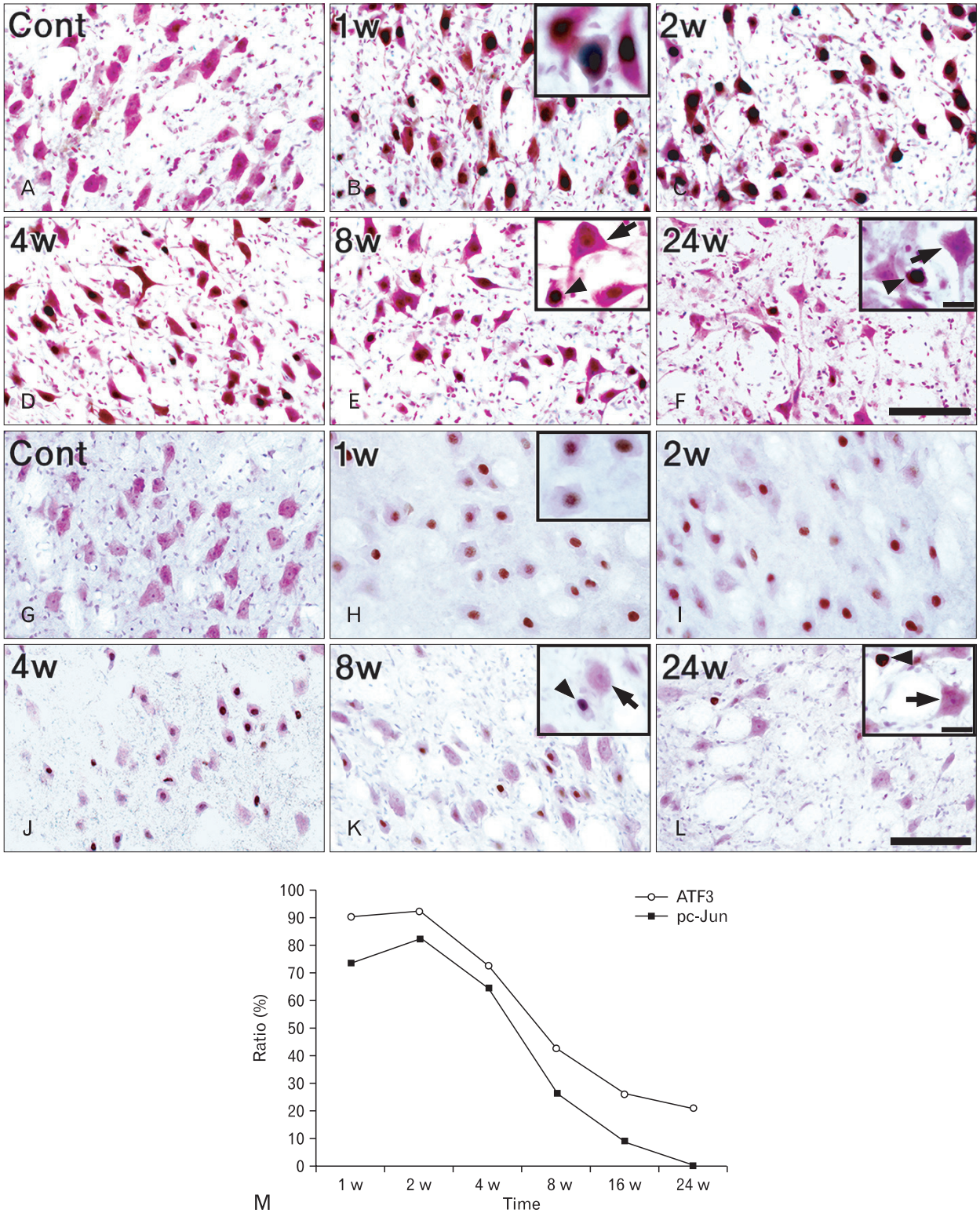

Fig. 2. (A-L) Localization of activating transcription factor 3 (ATF3) (A-F) and phosphorylated c-Jun (pc-Jun) (G-L) in axotomized facial motoneurons. (A, G) Contralateral, (B-F, H-L) ipsilateral side. Both ATF3 and pc-Jun were localized in the nuclei of numerous, normal-sized neurons by 2 weeks (w) post-lesion (B, C, H, I), then the numbers of ATF3- and pc-Jun-positive nuclei decreased progressively (D-F, J-L). At later time points, long-lasting activation of ATF3 and c-Jun was found predominantly in degenerating neurons with severely shrunken soma and condensed nuclei (arrowheads in insets of E, F, K, L) but not in neurons with normal morphology and soma size (arrows in insets of E, F, K, L). Cont, contralateral. Scale bars in (F, L)=100 μm (A-L); insets of (F, L)=20 μm (B, E, F, H, K, L). (M) Percentages of ATF3- and pc-Jun-positive neurons compared to the corresponding ipsilateral facial motoneurons.

http://dx.doi.org/10.5115/acb.2011.44.3.226

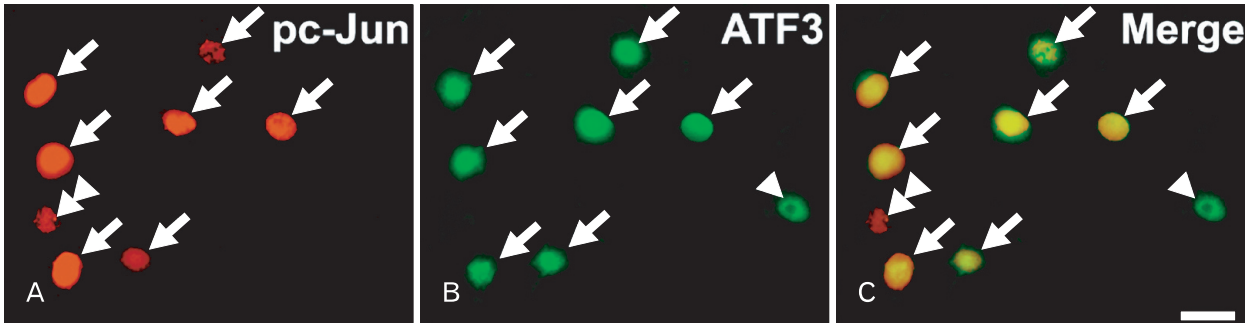

Fig. 3. Co-localization of activating transcription factor 3 (ATF3) and phosphorylated c-Jun (pc-Jun) in the axotomized facial motoneurons at 2 weeks post-lesion. ATF3 and pc-Jun were predominantly co-localized in the same neurons (arrows), with the exception of a few cells that were either pc-Jun-positive (double arrowheads) or ATF3-positive (arrowheads). Scale bar=20 μm.

4D).

Retrograde tracing with FG was performed at 2 wpl to obtain a more detailed spatial relationship between activated microglia and axotomized facial motoneurons. In these animals, various parts of some axotomized neurons were clearly identified by FG immunohistochemistry. Double labeling of FG with OX6 revealed that OX6-positive microglia simultaneously adhered to axons, dendrites, and cell bodies of FG-positive, axotomized facial motoneurons (Fig. 4G-I).

Double immunohistochemistry for ED1 and OX6 was performed to identify whether the OX6-positive microglia were phagocytic (Fig. 5A-F). Double labeling revealed that all OX6-positive microglia contained numerous ED1-positive particles (arrows in Fig. 5A-F), demonstrating that OX6-positive, activated microglia retain phagocytic activity. Additionally, to deduce the functional significance of ATF3 and pc-Jun, the spatial relationship between activated microglia and axotomized facial motoneurons was examined by triple labeling of pc-Jun, NeuN, and OX6 (Fig. 5G-I). This experiment clearly demonstrated that axotomized facial motoneurons characterized by nuclear phosphorylation of c-Jun were undergoing active phagocytosis by OX6-positive microglia (arrows in Fig. 5H, I).

Discussion

The survival rates of injured neurons in the central nucleus branching into peripheral nerves are highly variable and depend upon the type of injury, distance from the injured site to the origin, and age of the animal. In general, the viability of facial motoneurons transected or crushed outside the skull in adult rats is much greater than the viability after an intracranial axotomy of the facial nerve [28], combined ricin/crush lesions outside the skull in adult rats [34], extracranial axotomy in newborn rats [30], or an extracranial axotomy in aging rats [27]. Some authors have proposed that an extracranial facial nerve axotomy in adult rats does not induce significant neuronal cell death but rather allows the affected motoneurons to regenerate [30, 31]. However, others have reported a significant reduction in the number of facial motoneurons following an extracranial axotomy in adult rats. Guntinas-Lichius et al. [26] found 22% neuronal cell death at 8 wpl and 41% at 16 wpl following an extracranial facial nerve axotomy, whereas Mattsson et al. [28] reported that 28% of the facial motoneurons were lost 4 weeks after an axotomy in adult rats. Furthermore, Johnson and Duberley [27] estimated that 17% and 25% of motoneurons undergo cell death by 3 months after a facial nerve transection in adult Fischer 344 and Wistar rats, respectively. The differences in the rates of cell death among different studies may result from differences in surgical procedures or animal strains. In our study, we noted a significant reduction in the number of facial motoneurons from 16 wpl, with a percentage of neuronal loss of 20.9% at 16 wpl and 34.8% at 24 wpl. This percentage was generally less than that reported in previous studies [26-28].

ATF3 and c-Jun are rapidly induced and activated by stressful stimuli such as nerve injury and then act as transcription factors. Induction and activation of ATF3 and/or c-Jun are involved in two opposing functions, i.e., neuronal cell death and regeneration, depending on the cell type or injury pattern [1, 8, 11, 16-18]. Prolonged activation of pc-Jun and/or ATF3 may be related to cell death in the CNS [4, 16, 18, 35]. However, the axotomy response of peripheral or central extrinsic neurons is very different from that of central intrinsic neurons [36]. ATF3 and/or pc-Jun may be involved

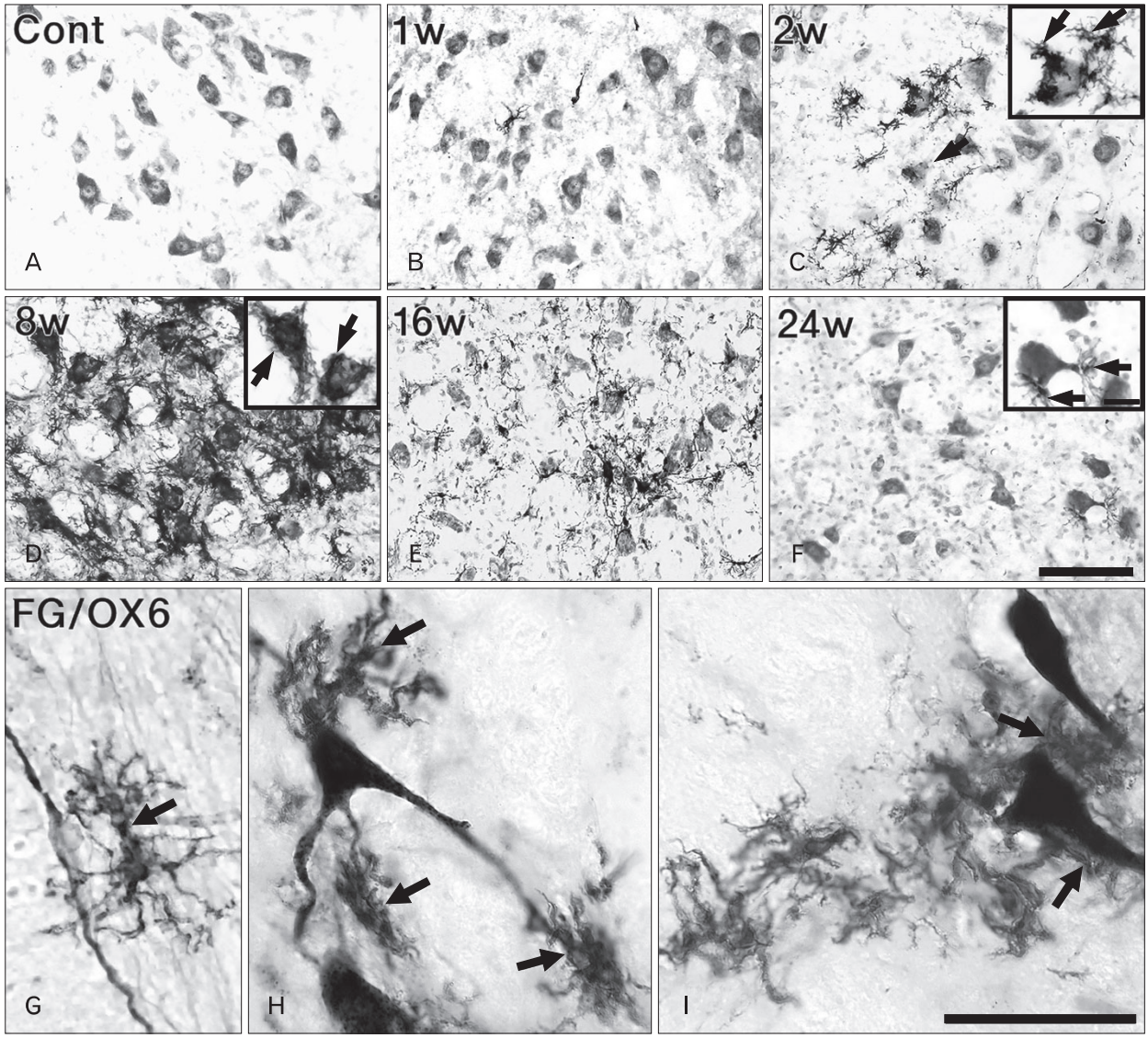

Fig. 4. (A-F) OX6 immunohistochemistry on the contralateral (A) and ipsilateral (B-F) sides. A few OX6-positive microglia were identified in the ipsilateral facial motor nucleus as early as 1 week (w) post-lesion (wpl) (B). The number of OX6-positive microglia increased significantly by 8 wpl (C, D) and subsequently decreased, but a few persisted up to 24 wpl (E, F). All OX6-positive microglia were ramified and closely adhered to or surrounded facial motoneurons (arrows in insets of C, D, F). (G-I) Double labeling of FluoroGold (FG) and OX6 at 2 wpl. OX6-positive microglia intimately adhered to the axon (arrow in G), dendrites (arrows in H), and cell bodies (arrows in I) of FG-positive, axotomized facial motoneurons. Cont, contralateral. Scale bars in (F)=100 μm (A-F), (I)=50 μm (G-I); inset of (F)=20 μm (C, D, F).

in neuronal regeneration, neuronal survival, or axonal sprouting and target reinnervation in the PNS, including the central extrinsic neurons [9, 25, 37, 38]. Lindwall and Kanje [37] proposed that injury-induced phosphorylation of c-Jun is accomplished by retrograde axonal transport of c-Jun N-terminal kinase (JNK) signaling components initiated by axonal damage, and that these activated transcription factors may, in turn, be responsible for the induction of proteins such as Hsp27, which are involved in neuronal survival and axonal sprouting. In addition, a study on JNK3-knockout mice and mice with a c-JunAA mutation (c-Jun with serines 63/73 replaced by nonphosphorylable alanines) demonstrated that these genes do not affect the survival of facial motoneurons following facial nerve axotomy, in contrast to the neuroprotective effects for axotomized DA neurons in the same animal strains [39].

In this study, we examined induction and activation of ATF3/c-Jun in axotomized facial motoneurons. Following

http://dx.doi.org/10.5115/acb.2011.44.3.226

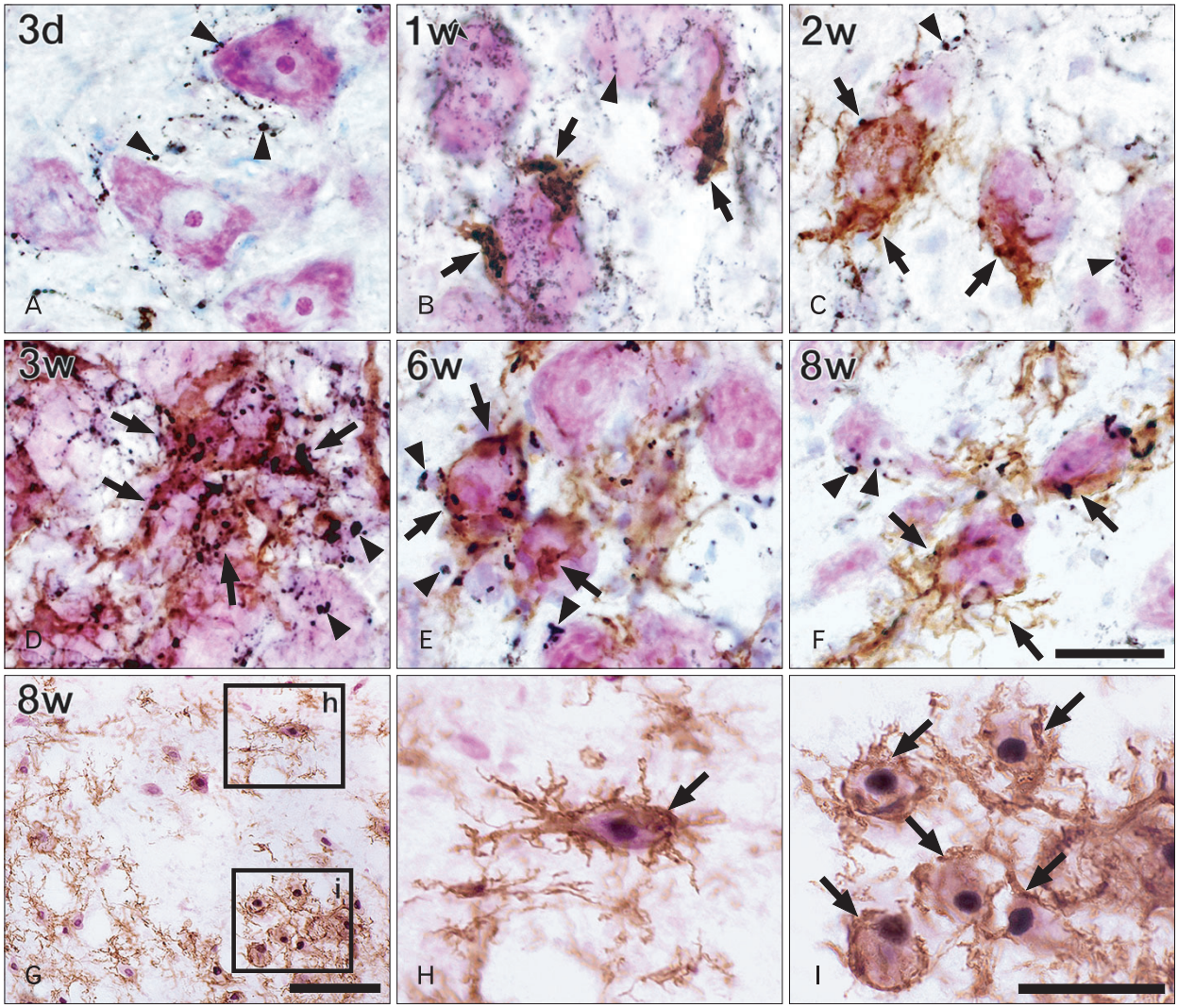

Fig. 5. (A-F) Double labeling of OX6 (brown) and ED1 (black) followed by counterstaining with cresyl violet in the facial motor nucleus at various time points. All OX6-positive microglia contained ED1-positive particles or spherical bodies (arrows). These microglia closely adhered to the degenerating facial motoneurons throughout all degenerative stages (A-F). Some microglia were labeled by ED1 but not by OX6 (arrowheads). (G-I) Triple labeling of neuronal nuclei (purple), phosphorylated c-Jun (black), and OX6 (brown) in the ipsilateral facial motor nucleus at 8 weeks post-lesion. Numerous pc-Jun-positive facial motoneurons were closely surrounded and phagocytosed by OX6-positive microglia (arrows in H, I). d, days; w, weeks. Scale bars in (F)=30 μm (A-F); (G)=100 μm; (I)=50 μm (H, I).

resection of the facial nerve outside the skull, ATF3 and pc-Jun were quickly and specifically induced in axotomized facial motoneurons. The percentage of ATF3-positive neurons compared to the ipsilateral facial motoneurons reached 90.9% at 1 wpl, and then decreased gradually to 21.0% at 24 wpl. The percentage of pc-Jun-positive neurons compared to the ipsilateral neurons increased up to 82.2% by 2 wpl and then progressively decreased to 0.1% by 24 wpl. Interestingly, while temporal profiles of the two IEG-positive neurons were very similar to each other, ATF3-positive neurons was always greater in number than pc-Jun-positive neurons.

We found that ATF3 and pc-Jun were localized in neurons with a normal size and shape by 2 wpl, but that at later time points, these IEGs were specifically found in the degenerating neurons with severely shrunken somas and condensed nuclei. These morphological features of ATF3- and pc-Jun-positive neurons indicate that they have already entered the execution stage, from which degenerating cells never return to the normal state [40]. Transcription factors, which normally function in neuronal survival or regeneration, are not likely to be specifically expressed in dying neurons with no possibility of survival. Therefore, our results strongly suggest that the

prolonged activation of ATF3/c-Jun in axotomized facial motoneurons may play a role in the signal transduction cascades related to neurodegeneration. In accordance with this, ipsilateral neurons with a normal size and morphology observed at later time points were neither ATF3- nor pc-Jun-positive, indicating that these IEGs had disappeared or had not been induced in these cells. Thus, the sharp decline in the number of ATF3- and pc-Jun-positive neurons after 2 wpl could be attributed to the disappearance of these IEGs from the surviving neurons, as well as to axotomy-induced neuronal cell death.

The functional effects of pc-Jun most likely depend on the cellular context and may be influenced by several cofactor proteins or by heterodimerization partners [3, 41]. ATF3 and c-Jun share a consensus sequence TGACTCA (TRE/AP-1 site) and form heterodimers or homodimers through a basic region/leucine zipper domain [42]. Heterodimerization of ATF3 and c-Jun has been demonstrated by *in vitro* co-immunoprecipitation studies [12]. This finding was supported by several *in vivo* co-immunolocalization studies. Concurrent induction/activation of ATF3 and c-Jun has been found in the dorsal root ganglion and spinal cord [5], retinal ganglion cells [25], and substantia nigra [4] after an axotomy. In the present study, we found that ATF3 and pc-Jun were co-localized in degenerating facial motoneurons in most cases. This finding suggests that putative pc-Jun/ATF3 heterodimers may be associated with axotomy-induced neuronal cell death cascades. Because the number of ATF3-positive neurons was somewhat greater than that of pc-Jun-positive neurons at all time points examined, ATF3 was presumed to have more potential to dimerize with proteins other than pc-Jun.

It has been suggested that resting microglia become activated but do not transform into phagocytes following transection [28, 30, 31] or crushing [34] of the facial nerve outside the skull in adult rats. These activated microglia proliferate and express strong OX42 immunoreactivity but lack monocyte/macrophage antigens recognized by OX41, ED1, ED2, Ki-M2R, or OX6. Several studies have suggested that the absence of ED1-positive, phagocytic microglia may reflect the fact that neuronal cell death following axotomy is minimal or that rat motoneurons do not die after facial nerve transection but rather regenerate in the adult facial nucleus [30, 31]. In these studies, survival times of the animals were only 6 [30] or 10 [31] days at the longest, limiting the available time for immunological examination with the antibodies for monocyte/macrophage antigens, including phagocytic marker ED1. In addition, Mattsson et al. [28] noted that despite the loss of approximately 28% of facial motoneurons at 4 weeks after extracranial facial nerve axotomy, no ED1-positive microglia were found in the facial nucleus.

In contrast to these studies, we found numerous OX6- and ED1-positive microglia in the facial motor nucleus following an extracranial facial nerve axotomy. A few OX6-positive microglia were found from 1 wpl, and their number increased dramatically by 8 wpl but then decreased. Double label experiments demonstrated that all OX6-positive microglia are ED1-positive, i.e., phagocytic. These OX6-positive microglia closely surrounded the axotomized facial motoneurons, suggesting that they ingested the neurons through active phagocytosis. Retrograde tracing with FG disclosed that OX6-positive microglia simultaneously adhered to various parts of axotomized facial motoneurons from the early stage of degeneration. The phagocytosis was particularly prominent at 8 wpl not only because so many OX6-positive microglia were engulfing the neurons (Fig. 4), but also because it was followed by a significant reduction in the number of axotomized facial motoneurons (Fig. 1). Triple immunohistochemistry for pc-Jun, NeuN, and OX6 clearly demonstrated that many neurons phagocytosed by OX6-positive microglia are pc-Jun-positive. This finding explains why both ATF3 and pc-Jun were localized in severely shrunken neurons at later time points but not in larger neurons with normal morphology.

Our results demonstrated that extracranial facial nerve axotomy induces neurodegenerative changes in facial motoneurons characterized by long-lasting nuclear ATF3 expression and c-Jun phosphorylation. Additionally, we confirmed that ATF3- and pc-Jun-positive, degenerating neurons were closely surrounded by activated microglia, implying active phagocytosis that was directly responsible for the neuronal loss in the ipsilateral facial motor nucleus. These intracellular events and microglial responses were largely identical to those found in the CNS following MFB transection [4, 22-24], except that the progress of neurodegeneration induced by the extracranial facial nerve axotomy was much slower than that induced by a MFB axotomy. Taken together, our results strongly support the idea that long-lasting activation of ATF3 and c-Jun, which are putative heterodimeric partners, may be involved in the intracellular signaling cascades resulting in neuronal cell death following an extracranial facial nerve axotomy.

http://dx.doi.org/10.5115/acb.2011.44.3.226

Acknowledgements

This work was supported by the Yonsei University Research Fund of 2005 (to Byung Pil Cho, YUWCM 2005-25). We would like to thank Mr. Dae Sung Park and Mr. Young Chul Kim, laboratory technicians in the Department of Anatomy, Yonsei University Wonju College of Medicine, for their excellent technical support.

References

1. Haas CA, Donath C, Kreutzberg GW. Differential expression of immediate early genes after transection of the facial nerve. Neuroscience 1993;53:91-9.
2. Sheng M, Greenberg ME. The regulation and function of c-fos and other immediate early genes in the nervous system. Neuron 1990;4:477-85.
3. Herdegen T, Skene P, Bähr M. The c-Jun transcription factor: bipotential mediator of neuronal death, survival and regeneration. Trends Neurosci 1997;20:227-31.
4. Song DY, Yang YC, Shin DH, Sugama S, Kim YS, Lee BH, Joh TH, Cho BP. Axotomy-induced dopaminergic neurodegeneration is accompanied with c-Jun phosphorylation and activation transcription factor 3 expression. Exp Neurol 2008;209:268-78.
5. Tsujino H, Kondo E, Fukuoka T, Dai Y, Tokunaga A, Miki K, Yonenobu K, Ochi T, Noguchi K. Activating transcription factor 3 (ATF3) induction by axotomy in sensory and motoneurons: a novel neuronal marker of nerve injury. Mol Cell Neurosci 2000;15:170-82.
6. Chen BP, Wolfgang CD, Hai T. Analysis of ATF3, a transcription factor induced by physiological stresses and modulated by gadd153/Chop10. Mol Cell Biol 1996;16:1157-68.
7. Hai T, Wolfgang CD, Marsee DK, Allen AE, Sivaprasad U. ATF3 and stress responses. Gene Expr 1999;7:321-35.
8. Kawauchi J, Zhang C, Nobori K, Hashimoto Y, Adachi MT, Noda A, Sunamori M, Kitajima S. Transcriptional repressor activating transcription factor 3 protects human umbilical vein endothelial cells from tumor necrosis factor-alpha-induced apoptosis through down-regulation of p53 transcription. J Biol Chem 2002;277:39025-34.
9. Nakagomi S, Suzuki Y, Namikawa K, Kiryu-Seo S, Kiyama H. Expression of the activating transcription factor 3 prevents c-Jun N-terminal kinase-induced neuronal death by promoting heat shock protein 27 expression and Akt activation. J Neurosci 2003;23:5187-96.
10. Hartman MG, Lu D, Kim ML, Kociba GJ, Shukri T, Buteau J, Wang X, Frankel WL, Guttridge D, Prentki M, Grey ST, Ron D, Hai T. Role for activating transcription factor 3 in stress-induced beta-cell apoptosis. Mol Cell Biol 2004;24:5721-32.
11. Mashima T, Udagawa S, Tsuruo T. Involvement of transcriptional repressor ATF3 in acceleration of caspase protease activation during DNA damaging agent-induced apoptosis. J Cell Physiol 2001;188:352-8.
12. Hai T, Curran T. Cross-family dimerization of transcription factors Fos/Jun and ATF/CREB alters DNA binding specificity. Proc Natl Acad Sci U S A 1991;88:3720-4.
13. Leah JD, Herdegen T, Bravo R. Selective expression of Jun proteins following axotomy and axonal transport block in peripheral nerves in the rat: evidence for a role in the regeneration process. Brain Res 1991;566:198-207.
14. Sommer C, Gass P, Kiessling M. Selective c-JUN expression in CA1 neurons of the gerbil hippocampus during and after acquisition of an ischemia-tolerant state. Brain Pathol 1995;5:135-44.
15. Dragunow M, Beilharz E, Sirimanne E, Lawlor P, Williams C, Bravo R, Gluckman P. Immediate-early gene protein expression in neurons undergoing delayed death, but not necrosis, following hypoxic-ischaemic injury to the young rat brain. Brain Res Mol Brain Res 1994;25:19-33.
16. Dragunow M, Young D, Hughes P, MacGibbon G, Lawlor P, Singleton K, Sirimanne E, Beilharz E, Gluckman P. Is c-Jun involved in nerve cell death following status epilepticus and hypoxic-ischaemic brain injury? Brain Res Mol Brain Res 1993;18:347-52.
17. Ferrer I, Olive M, Ribera J, Planas AM. Naturally occurring (programmed) and radiation-induced apoptosis are associated with selective c-Jun expression in the developing rat brain. Eur J Neurosci 1996;8:1286-98.
18. Oo TF, Henchcliffe C, James D, Burke RE. Expression of c-fos, c-jun, and c-jun N-terminal kinase (JNK) in a developmental model of induced apoptotic death in neurons of the substantia nigra. J Neurochem 1999;72:557-64.
19. Crocker SJ, Lamba WR, Smith PD, Callaghan SM, Slack RS, Anisman H, Park DS. c-Jun mediates axotomy-induced dopamine neuron death in vivo. Proc Natl Acad Sci U S A 2001;98:13385-90.
20. Anderson AJ, Cummings BJ, Cotman CW. Increased immunoreactivity for Jun- and Fos-related proteins in Alzheimer's disease: association with pathology. Exp Neurol 1994;125:286-95.
21. Martín G, Seguí J, Díaz-Villoslada P, Montalbán X, Planas AM, Ferrer I. Jun expression is found in neurons located in the vicinity of subacute plaques in patients with multiple sclerosis. Neurosci Lett 1996;212:95-8.
22. Cho BP, Song DY, Sugama S, Shin DH, Shimizu Y, Kim SS, Kim YS, Joh TH. Pathological dynamics of activated microglia following medial forebrain bundle transection. Glia 2006;53:92-102.
23. Cho BP, Sugama S, Shin DH, DeGiorgio LA, Kim SS, Kim YS, Lim SY, Park KC, Volpe BT, Cho S, Joh TH. Microglial phagocytosis of dopamine neurons at early phases of apoptosis. Cell Mol Neurobiol 2003;23:551-60.
24. Sugama S, Cho BP, Degiorgio LA, Shimizu Y, Kim SS, Kim YS, Shin DH, Volpe BT, Reis DJ, Cho S, Joh TH. Temporal

and sequential analysis of microglia in the substantia nigra following medial forebrain bundle axotomy in rat. Neuroscience 2003;116:925-33.
25. Takeda M, Kato H, Takamiya A, Yoshida A, Kiyama H. Injury-specific expression of activating transcription factor-3 in retinal ganglion cells and its colocalized expression with phosphorylated c-Jun. Invest Ophthalmol Vis Sci 2000;41:2412-21.
26. Guntinas-Lichius O, Neiss WF, Gunkel A, Stennert E. Differences in glial, synaptic and motoneuron responses in the facial nucleus of the rat brainstem following facial nerve resection and nerve suture reanastomosis. Eur Arch Otorhinolaryngol 1994;251:410-7.
27. Johnson IP, Duberley RM. Motoneuron survival and expression of neuropeptides and neurotrophic factor receptors following axotomy in adult and ageing rats. Neuroscience 1998;84:141-50.
28. Mattsson P, Meijer B, Svensson M. Extensive neuronal cell death following intracranial transection of the facial nerve in the adult rat. Brain Res Bull 1999;49:333-41.
29. Gehrmann J, Mies G, Bonnekoh P, Banati R, Iijima T, Kreutzberg GW, Hossmann KA. Microglial reaction in the rat cerebral cortex induced by cortical spreading depression. Brain Pathol 1993;3:11-7.
30. Graeber MB, López-Redondo F, Ikoma E, Ishikawa M, Imai Y, Nakajima K, Kreutzberg GW, Kohsaka S. The microglia/macrophage response in the neonatal rat facial nucleus following axotomy. Brain Res 1998;813:241-53.
31. Graeber MB, Streit WJ, Kreutzberg GW. Axotomy of the rat facial nerve leads to increased CR3 complement receptor expression by activated microglial cells. J Neurosci Res 1988;21:18-24.
32. Paxinos G, Watson C. The rat brain in stereotaxic coordinates. 4th ed. San Diego: Academic Press; 1998.
33. Damoiseaux JG, Döpp EA, Calame W, Chao D, MacPherson GG, Dijkstra CD. Rat macrophage lysosomal membrane antigen recognized by monoclonal antibody ED1. Immunology 1994;83:140-7.
34. Streit WJ, Kreutzberg GW. Response of endogenous glial cells to motor neuron degeneration induced by toxic ricin. J Comp Neurol 1988;268:248-63.
35. Dragunow M, Preston K. The role of inducible transcription factors in apoptotic nerve cell death. Brain Res Brain Res Rev 1995;21:1-28.
36. Barron KD. The axotomy response. J Neurol Sci 2004;220:119-21.
37. Lindwall C, Kanje M. Retrograde axonal transport of JNK signaling molecules influence injury induced nuclear changes in p-c-Jun and ATF3 in adult rat sensory neurons. Mol Cell Neurosci 2005;29:269-82.
38. Raivich G, Bohatschek M, Da Costa C, Iwata O, Galiano M, Hristova M, Nateri AS, Makwana M, Riera-Sans L, Wolfer DP, Lipp HP, Aguzzi A, Wagner EF, Behrens A. The AP-1 transcription factor c-Jun is required for efficient axonal regeneration. Neuron 2004;43:57-67.
39. Brecht S, Kirchhof R, Chromik A, Willesen M, Nicolaus T, Raivich G, Wessig J, Waetzig V, Goetz M, Claussen M, Pearse D, Kuan CY, Vaudano E, Behrens A, Wagner E, Flavell RA, Davis RJ, Herdegen T. Specific pathophysiological functions of JNK isoforms in the brain. Eur J Neurosci 2005;21:363-77.
40. Pittman RN, Messam CA, Mills JC. Asynchronous death as a characteristics feature of apoptosis. In: Koliatsos VE, Ratan RR, editors. Cell Death and Diseases of the Nervous System. Totowa: Hamana Press; 1998. p.29-44.
41. Reimold AM, Grusby MJ, Kosaras B, Fries JW, Mori R, Maniwa S, Clauss IM, Collins T, Sidman RL, Glimcher MJ, Glimcher LH. Chondrodysplasia and neurological abnormalities in ATF-2-deficient mice. Nature 1996;379:262-5.
42. Karin M, Liu Z, Zandi E. AP-1 function and regulation. Curr Opin Cell Biol 1997;9:240-6.